

Strong 1.3–1.5 μm luminescence from Ge/Si self-assembled islands in highly confining microcavities on silicon on insulator

M. El Kurdi, S. David, P. Boucaud,^{a)} C. Kammerer, X. Li, V. Le Thanh,^{b)} S. Sauvage, and J.-M. Lourtioz

Institut d'Électronique Fondamentale UMR CNRS 8622 Bâtiment 220, Université Paris-Sud, 91405 Orsay, France

(Received 5 February 2004; accepted 1 April 2004)

We report dramatic enhancement of 1.3–1.5 μm room-temperature emission from self-assembled Ge/Si islands in highly confining microcavities on silicon on insulator. The microcavities are fabricated either by creating defects in two-dimensional silicon-based photonic crystals or by etching the silicon layer in order to form isolated micropillars. The optical emission is characterized by nonlinear evolution with pump power, the nonlinearity being more pronounced as the microcavity size is reduced. Both the nonlinearity and luminescence extraction are enhanced in photonic crystals with large air filling factors. The results are interpreted in terms of carrier localization. The luminescence extracted is more than two orders of magnitude higher than that of the unprocessed sample while it is 1% that of a single InGaAs quantum well. This system appears to be a promising alternative for microsources on silicon at telecommunication wavelengths that are fully compatible with silicon-based processing technologies. © 2004 American Institute of Physics.

[DOI: 10.1063/1.1753655]

I. INTRODUCTION

Getting light efficiently out of silicon has always been a long standing goal for many researchers. The combination of optical functionalities integrated on a silicon chip should allow the development of devices at low cost for multimedia markets and address some key issues for inter- and intrachip optical interconnections. The increase of quantum efficiency of a silicon integrated source requires specific approaches in order to bypass the inefficiency associated with an indirect gap semiconductor.¹ The first approach aims at limiting the presence of defects or surface states which lead to nonradiative recombination. Proper surface passivation is required in order to decrease parasitic nonradiative recombination of the charge carriers. This surface passivation can be combined with carrier localization that prevents diffusion of the carriers towards nonradiative states. The validity of this approach was recently demonstrated with the development of efficient silicon-based light emitting diodes operating at room temperature where carriers in silicon are confined by the strain fields of dislocation loops intentionally introduced into the structure.² Collection of emitted photons is also an issue, as is the case for III–V semiconductors, because of the high refractive index of the materials. The standard approach, also used for III–V materials, is thus based on texturing the surface of the material which allows better coupling to vertical radiation of the emitted photons. This approach was also reported recently in the case of silicon diodes operating at room temperature.^{3,4} However light emitting diodes based on the phonon assisted optical recombination in silicon only op-

erate around 1.15 μm at room temperature. The shift of emission towards longer wavelengths, and in particular to 1.3 and 1.55 μm telecommunication wavelengths, requires the introduction of impurities and specific defect centers like carbon,⁵ rare-earth atoms codoped with oxygen⁶ or materials that are fully compatible with silicon-based technology like silicon germanium alloys.⁷

Here we show that a combination of Ge/Si self-assembled islands with microcavities obtained either with two-dimensional photonic crystals on silicon-on-insulator (SOI) substrates or isolated micropillars leads to enhanced emission at room temperature which covers the 1.3–1.55 μm spectral range. The Ge/Si self-assembled islands offer two main advantages. The first advantage is associated with the rich Ge content of the islands and the band gap reduction associated with the strain field of islands buried in the silicon matrix. Both features lead to band edge recombination which covers the 1.3–1.55 μm spectral range. The second advantage is associated with carrier localization in the islands which limits the diffusion to nonradiative states and favors radiative recombination of the carriers. Because of the indirect band gap and the long recombination time of carriers, high carrier densities can be achieved in this system for moderate optical excitation.⁸ In this work, we have investigated samples periodically patterned into two-dimensional photonic crystals⁹ on SOI and defect microcavities obtained by etching silicon film deposited on the oxide insulator. The interest in using photonic crystals is their capability to be integrated into photonic circuits and their capacity to modify the density of confined optical modes and the pattern of radiation of an emitter. The emission at specific wavelengths can be enhanced by coherent scattering of light to the continuum lying above the light line.¹⁰ The emission can also be enhanced at resonant mode frequencies by using photonic

^{a)}Electronic mail: philippe.boucaud@ief.u-psud.fr

^{b)}Present address: Centre de Recherche sur les Mécanismes de la Croissance Cristalline, CRMC2-CNRS, Campus de Luminy, Case 913, 13009 Marseille, France.

crystals microcavities. We show that blocking of carrier diffusion in two-dimensional photonic crystals on SOI characterized by a large r/a coefficient (hole radius divided by the periodicity) leads to strong nonlinear emission of Ge islands. A similar effect is observed with micropillar structures.

II. SAMPLES AND EXPERIMENTAL SETUP

The samples studied were grown on a SOI substrate with a $3.5\ \mu\text{m}$ thick, buried oxide layer and a $0.2\ \mu\text{m}$ thick silicon layer on top of the oxide. The active layer, consisting of three Ge/Si self-assembled island layers separated by $20\ \text{nm}$ silicon barriers, was grown by low pressure chemical vapor deposition.¹¹ The islands had a typical base width of $120\ \text{nm}$, height of $10\ \text{nm}$ and density of around $1 \times 10^9\ \text{cm}^{-2}$. The total thickness of the waveguide core including the Ge/Si island layers was $0.3\ \mu\text{m}$. This value is sufficiently small to ensure single-mode waveguiding at $1.5\ \mu\text{m}$ once the whole photonic crystal structure is processed. The two-dimensional photonic crystals and microcavities were defined by electron beam lithography with a triangular lattice of holes of $0.5\ \mu\text{m}$ period. The pattern was transferred into the guiding silicon–Ge/Si multilayers using reactive ion etching. The holes drilled into the silicon–Ge/Si multilayers down to the buried oxide layer had diameters of between 0.3 and $0.45\ \mu\text{m}$. Different hexagonal cavities ($H2$ – $H3$ and $H5$) were inserted into the photonic crystal by omitting to drill a defined number of air holes.¹² We have also analyzed some $H2$ cavities for which the periodic patterning surrounding the cavities was partially removed. These cavities, which are intermediate between micropillars and standard defect microcavities in two-dimensional photonic crystals, are labeled as $H2^*$ in the following. Micropillars obtained by etching the silicon film on top of the oxide were also investigated. The photoluminescence was measured at room temperature with a continuous wave Ar⁺ pump laser beam in a normal incidence configuration. The excitation and photoluminescence beams were focused and collected with the same objective of 0.65 numerical aperture. The excitation spot is around $2\ \mu\text{m}$. The luminescence was filtered within a $100\ \mu\text{m}$ diameter pinhole located at the focal point of a $15\ \text{cm}$ focal lens. The luminescence was dispersed by a monochromator and detected with a liquid-nitrogen cooled germanium detector using standard lock-in techniques.

III. RESULTS

Figure 1 shows the power dependence of the photoluminescence at room temperature for a $H3$ microcavity. A top view scanning electron micrograph of the cavity is shown in the inset. For hole diameters of $0.4\ \mu\text{m}$, the two-dimensional photonic crystal exhibits a forbidden band in transverse electric (TE) polarization between 0.6 and $1\ \text{eV}$.¹³ For the $H3$ microcavity, a fairly great number of defect modes associated with light confinement appear in the photonic band gap. The modes above the light line can be coupled to the free space continuum of modes. In the region free of photonic crystals, the island photoluminescence is resonant at room temperature around $0.91\ \text{eV}$ with a full width at half maximum of $0.11\ \text{eV}$. Two distinct features are evidenced in

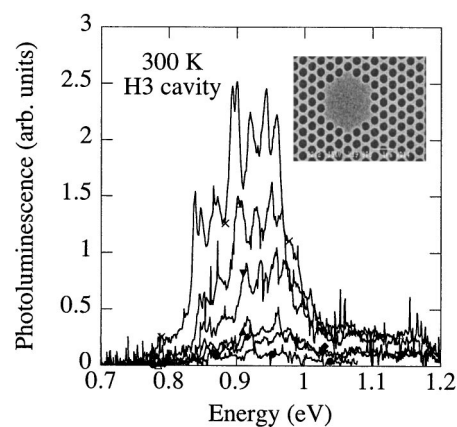


FIG. 1. Room temperature photoluminescence of a $H3$ microcavity containing Ge/Si self-assembled islands. The photoluminescence is shown as a function of the excitation power. The excitation power increases from 14 to $27\ \text{mW}$ (14 mW closed circles; 16 mW diamonds; 20 mW closed triangles; 22 mW inverted triangles; 24 mW triangles; 27 mW crosses). The inset shows a scanning electron micrograph of the $H3$ microcavity. The periodicity of the triangular pattern is $0.5\ \mu\text{m}$. The diameter of the air hole is $0.4\ \mu\text{m}$.

Fig. 1. When the photoluminescence is collected from the microcavity, it exhibits resonances, which are associated with the defect modes of the microcavity. The choice of microcavity and photonic crystal parameters including the cavity size and the hole diameters provides a tool by which to tune the emission to specific wavelengths.¹³ Besides, we want to note that the luminescence in this silicon-based system is not quenched by electronic defect states generated by the etching process at the interfaces as is often the case with III–V materials. The second key feature shown in Fig. 1 is the dramatic increase of emitted photoluminescence as a function of the excitation power density. This power dependence is characterized by laser-like emission with threshold around $10\ \text{mW}$ for this structure. Superlinear emission with smaller superlinearity has already been reported for silicon devices, either in the case of bare silicon samples,¹⁴ p – n silicon diodes,² p -metal–oxide–semiconductor (MOS) silicon diodes¹⁵ or silicon samples that contain a high density of defects.¹⁶ In the latter cases, the nonlinearity scales as the square of the excitation density while in the present work the nonlinearity is much stronger. The striking feature in this work is that the nonlinear behavior can be controlled by the cavity size. We want to emphasize that the enhancement covers the whole spectral range of emission and is not limited to a specific wavelength. Meanwhile, the photoluminescence exhibits a slight redshift as the power excitation density is increased.

Figure 2 shows the power dependence of the photoluminescence measured at room temperature for different samples. The first sample (shown by triangles) corresponds to vertical stacking of Ge islands in a silicon matrix. The photoluminescence intensity measured at the peak of the photoluminescence island is characterized by a sublinear dependence with the excitation power, as usually observed. The second sample (shown by closed circles) corresponds to Ge islands deposited on a silicon on insulator substrate, i.e., the sample investigated without processing. The presence of the

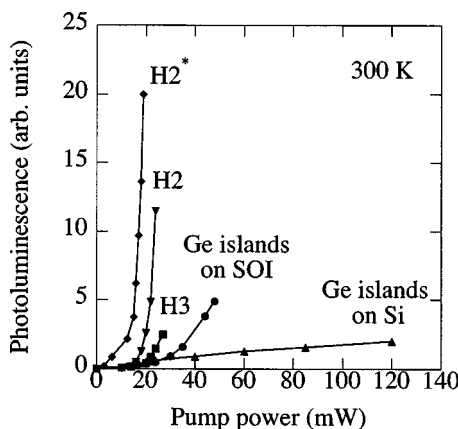


FIG. 2. Peak photoluminescence amplitude at room temperature as a function of the excitation power. The triangles correspond to Ge islands embedded in a silicon matrix. Closed circles correspond to Ge islands deposited on top of a silicon-on-insulator substrate. $H3$ (squares) and $H2$ (inverted triangles) correspond to microcavities embedded in two-dimensional photonic crystals. The curve labeled $H2^*$ corresponds to an $H2$ microcavity with a partially removed photonic crystal environment (diamonds).

silicon oxide layer blocks diffusion of the carrier the substrate and thus leads to an increase of local carrier density. This local carrier density increase leads to superlinear emission which dominates above 30 mW compared to standard Ge islands on silicon. If we now turn to the case of $H3$ and $H2$ microcavities, we observe that the onset of nonlinear emission occurs at smaller excitation densities with a threshold around 10 mW for the $H2$ microcavity. Moreover, the slope that characterizes the emission above threshold increases for smaller cavities. Both effects lead to dramatic enhancement of the emission at room temperature as the cavity size is reduced. The presence of photonic crystal patterning and the photonic band gap is not necessary to observe the enhanced luminescence. The luminescence of the cavities with a partially removed photonic crystal environment also leads to great enhancement, as shown in Fig. 2 by the curve labeled $H2^*$. Regular periodical patterning around the cavities is thus not required to observe the enhanced luminescence. We note that the resonant character of the emission is lost in this case, probably because of an increase in photon loss: the photoluminescence spectrum is similar to that of the original unprocessed structure [see Fig. 3(b)]. The integrated emitted power of the $H2^*$ cavity is around 1 μW . Enhanced emission was also observed in micropillars with micrometer-size diameters obtained by etching the silicon film containing Ge islands down to the oxide layer. We should emphasize that the emission remains much weaker when optically exciting the periodic structure of the photonic crystal instead of the microcavity. But we did not find strong nonlinearity in that case. This enhanced emission is also only observed for photonic crystals with large air filling factors and a hole radius-to-period ratio, r/a , larger than 0.35.

IV. DISCUSSION

We now discuss the origin of the enhanced luminescence. Below a critical temperature and above a threshold carrier density given by the Mott criterion, the luminescence

in an indirect band gap material like silicon corresponds to recombination of an electron hole droplet.¹⁷ As the temperature is increased, a phase transition occurs and the band edge luminescence of silicon corresponds to electron hole plasma recombination with a characteristic spectral shape.¹⁸ The critical temperature and densities in silicon that correspond to condensation are 27 K and 10^{18} cm^{-3} .¹⁷ In the present work, the dramatic enhancement of the photoluminescence is associated with the high electron and hole carrier densities that can be achieved in this system. First, the buried SiO_2 barrier blocks carrier diffusion to the substrate.¹⁹ Second, lateral patterning of the structure partially inhibits lateral diffusion of the carriers, thus leading to a local very dense electron hole plasma. This three-dimensional localization of the carriers counterbalances the effect usually observed in focused illumination where a large fraction of carriers diffuse away from the illuminated area. In photonic crystals, blocking of carrier diffusion is even more pronounced when the air filling factor of the crystal increases. The high plasma density provides an additional scattering mechanism of the carriers to the zone center, thus enhancing the photoluminescence.²⁰ It is worth mentioning that enhancement of the photoluminescence is only observed for recombination in the Ge islands and not in the silicon matrix. This feature *rules out thermal effects and blackbody radiation* as the origin of the enhanced luminescence since the emittance of the silicon matrix would be enhanced in that case. Moreover, such enhanced luminescence was not observed for a simple silicon-on-oxide layer. The trapping of holes in Ge islands and, thus, their limited diffusion to parasitic nonradiative recombination centers in conjunction with more favorable radiative recombination induced by Coulomb interactions, are thus key features in explaining the nonlinear emission. At high carrier densities, strong band bending occurs around the Ge/Si heterostructure.²¹ Since the recombination is spatially indirect for Ge/Si islands between electrons in the silicon matrix and the hole trapped in the islands, band bending can enhance the overlap between electron and hole wave functions, thus enhancing in turn the luminescence efficiency. We emphasize that the buried oxide layer blocks carrier diffusion and thus provides enhanced carrier localization in the silicon matrix. The thickness of the silicon matrix is however too large to result in quantum confinement of the carriers. Quantum confinement of carriers only results from the band lineup between the SiGe islands and the surrounding Si. Coulomb interaction provides an additional mechanism for carrier localization around islands.

Finally, we have compared the emission of Ge/Si islands in photonic microcavities with the emission of a III-V sample containing a high quality InGaAs quantum well. The latter sample consists of a single 7 nm thick $\text{In}_{0.38}\text{Ga}_{0.62}\text{As}$ quantum well surrounded by 100 nm thick GaAs barriers and 25 nm thick $\text{Al}_{0.3}\text{Ga}_{0.7}\text{As}$ barriers. The same experimental setup was used to measure the room temperature photoluminescence of this reference sample. Figure 3(a) shows a comparison at room temperature of the power dependence of the photoluminescence of the unprocessed InGaAs quantum well sample compared to the Ge/Si $H2$ isolated cavity. Figure 3(b) shows a comparison between the spectral shape of both

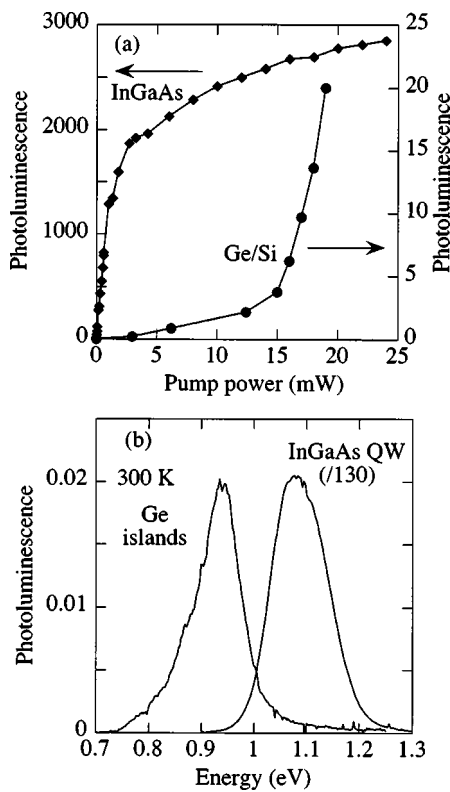


FIG. 3. (a) Comparison between the power dependence of the photoluminescence amplitude of a $H2^*$ microcavity and the photoluminescence of an InGaAs quantum well surrounded by AlGaAs barriers. (b) Spectral shape of both emissions.

emissions. The power dependence of the photoluminescence between both samples differs. At room temperature, the peak photoluminescence amplitude of the InGaAs quantum well sample increases linearly up to 1 mW and saturates at high excitation power. For excitation power of 20 mW, the photoluminescence efficiency of the Ge/Si microcavities is lower by around two orders of magnitude compared to the “bare” III–V sample. We note that the excitation delivered by the argon ion laser is more efficiently absorbed in the GaAs matrix compared to silicon. Despite the lower efficiency, embedding Ge islands inside microcavities appears to be a promising alternative to bridge the gap between the optical efficiency of IV–IV and III–V materials.

V. CONCLUSION

In conclusion, we have shown that the incorporation of Ge islands in microcavities leads to significant room tem-

perature photoluminescence enhancement in the 1.3–1.55 μm spectral range. This enhancement can reach two orders of magnitude compared to the unprocessed sample. The enhancement of Ge island optical recombination is attributed to carrier localization in the cavity and around the islands, leading to an increase in the probability of internal radiative recombination. Microcavities with Ge/Si self-assembled islands are a challenging alternative to the development of microsources operating at telecommunication wavelengths that can be monolithically integrated on silicon.

ACKNOWLEDGMENTS

The authors thank Isabelle Sagnes for providing the InGaAs quantum well sample.

- ¹L. Tsybeskov, K. L. Moore, D. G. Hall, and P. M. Fauchet, Phys. Rev. B **54**, R8361 (1996).
- ²W. L. Ng, M. A. Lourenço, R. M. Gwilliam, S. Ledain, G. Shao, and K. P. Homewood, Nature (London) **410**, 192 (2001).
- ³M. A. Green, J. Zhao, A. Wang, P. J. Reece, and M. Gal, Nature (London) **412**, 805 (2001).
- ⁴T. Trupke, J. Zhao, A. Wang, R. Corkish, and M. A. Green, Appl. Phys. Lett. **82**, 2996 (2003).
- ⁵L. T. Canham, K. G. Barraclough, and D. J. Robbins, Appl. Phys. Lett. **51**, 1509 (1987).
- ⁶G. Franzo, F. Priolo, S. Coffa, A. Polman, and A. Carnera, Appl. Phys. Lett. **64**, 2235 (1994).
- ⁷D. J. Robbins, L. T. Canham, S. J. Barnett, A. D. Pitt, and P. Calcott, J. Appl. Phys. **71**, 1407 (1992).
- ⁸M. Ruff, M. Fick, R. Lindner, U. Rössler, and R. Helbig, J. Appl. Phys. **74**, 267 (1993).
- ⁹E. Yablonovitch, Phys. Rev. Lett. **58**, 2059 (1987).
- ¹⁰S. Fan, P. R. Villeneuve, J. D. Joannopoulos, and E. F. Schubert, Phys. Rev. Lett. **78**, 3294 (1997).
- ¹¹V. Le Thanh, V. Yam, P. Boucaud, F. Fortuna, C. Ulysse, D. Bouchier, L. Vervoort, and J. M. Lourtioz, Phys. Rev. B **60**, 5851 (1999).
- ¹²H. Benisty *et al.*, J. Lightwave Technol. **17**, 2063 (1999).
- ¹³S. David, M. El Kurdi, P. Boucaud, A. Chelnokov, V. Le Thanh, D. Bouchier, and J. M. Lourtioz, Appl. Phys. Lett. **83**, 2509 (2003).
- ¹⁴D. Guidotti, J. S. Batchelder, A. Finkel, and J. A. Van Vechten, Phys. Rev. B **38**, 1569 (1988).
- ¹⁵C. W. Liu, M. H. Lee, M.-J. Chen, I. C. Lin, and C.-F. Lin, Appl. Phys. Lett. **76**, 1516 (2000).
- ¹⁶E. O. Sveinbjörnsson and J. Weber, Appl. Phys. Lett. **69**, 2686 (1996).
- ¹⁷J. Shah, M. Combescot, and A. H. Dayem, Phys. Rev. Lett. **38**, 1497 (1977).
- ¹⁸Ya. Pokrovskii, Phys. Status Solidi A **11**, 385 (1972).
- ¹⁹M. Tajima and S. Ibuka, J. Appl. Phys. **84**, 2224 (1998).
- ²⁰B. E. Sernelius, Phys. Rev. B **39**, 10825 (1989).
- ²¹T. Baier, U. Mantz, K. Thonke, R. Sauer, F. Schäffler, and H. J. Herzog, Phys. Rev. B **50**, 15191 (1994).